Visual Abstract

The proposition of analytical expression H_M–($\sqrt{P}/S$) in microindentation pile-up deformation mode

D.-E. Semsoum
LGIDD, Department of Mechanical Engineering, Mustapha Stambouli University of Mascara, 29000, Algeria.
djameleddine.semsoum@univ-mascara.dz

S. Habibi*
Laboratory of Industrial Engineering and Sustainable Development (LGIDD, Department of Mechanical Engineering, Ahmed Zabana University of Relizane, 48000, Algeria.
habibismr@yahoo.com

S. Benaissa, H. Merzouk
LGIDD, Department of Mechanical Engineering, Mustapha Stambouli University of Mascara, 29000, Algeria.
soufiane.benaissa@univ-mascara.dz, hassen.merzouk@univ-mascara.dz

ABSTRACT. In this article, the characteristic curves of microindentation measured on Cu99 were analyzed on the basis of the analytical expression proposed by Habibi et al. (J. Mater. Res, 2021, 36 (15): 3074-3085). The ratio of applied load to square displacement, $P/(h+h_0)^2$, was discovered to be non-constant during the loading segment of the microindentation test. An empirical expression for the determination of Martens hardness as a function of indentation load, contact stiffness, and reduced modulus of elasticity by analyzing indentation load curves has been proposed for pile-up mode strain with the corrections imposed by the tip defect, the compliance of the instrument, and the axial axisymmetry coefficient of the Vickers indenter. The results from microindentation tests on this examined ductile material show excellent agreement.

KEYWORDS. Microindentation; Martens hardness; Pile-up; Empirical; Cu99.

OPEN ACCESS

Citation: Semsoum, D.-E., Habibi, S., Benaissa, S., Merzouk, The proposition of analytical expression HM–(√P/S) in microindentation pile-up deformation mode, Frattura ed Integrità Strutturale, 60 (2022) 407-415.

Received: 05.10.2021
Accepted: 05.03.2022
Online first: 17.03.2022
Published: 01.04.2022

Copyright: © 2022 This is an open access article under the terms of the CC-BY 4.0, which permits unrestricted use, distribution, and reproduction in any medium, provided the original author and source are credited.

INTRODUCTION

Many scientific investigations [1–5] reveal that the load curve derived from indentation experiments may be correctly characterized by the following power law:

$$P=\Lambda h^2 \quad (1)$$

Thus, the load P is equal to a constant ʎ times the square of the indentation depth h. This equation was developed by (Hainsworth et al., 1996) [1] to refine a previous approach by Loubet et al. [2], a three-dimensional finite element calculation (Zeng and Rowcliffe, 1996) [3], a dimensional analysis and finite element calculations (Cheng and Cheng, 1998) [4]. This relation (1) was used as a basis for the calibration of the indent radius and the calibration of the compliance (Sun et al., 1999) [5]. The value of the constant ʎ depends on the geometry of the tip and the properties of the indented material. Malzbender et al. [6] attempted to develop and refine a previous approach by Hainsworth et al. [1] Originally suggested to express P-h², they derived Eqn. (2) after analyzing indentation load-displacement curves measured on a wide range of different materials.

$$P = E_r \left(\frac{1}{\sqrt{c}} \sqrt{\frac{E_r}{H}} + \varepsilon \sqrt{\frac{\pi}{4}} \sqrt{\frac{H}{E_r}} \right)^{-2} \left(h_m + h_0 \right)^2 \tag{2}$$

The authors [6] formulated the expression (2) of Young's modulus (E) and of the hardness of the material (H) by indentation, for the mode of deformation in sink-in by indentation and they consider that the ratio $P/(h+h_0)^2$ is constant. However, the authors, Habibi et al. [7] implemented a new analytical expression to predict the behavior of the material from H and E exclusively for the strain under the indenter in pile-up mode, taking into account the correction of the tip defect. This experimental relationship has been approved on the basis of a range of materials from different families. This expression is shown in Eq. (3) as follows:
Where, E and H have been calculated via indentation, and the authors [6] consider that the ratio $P/(h+h_0)^2$ is a constant in sink-in deformation. As a result of the tip fault being corrected, the authors Habibi et al. [7] devised a new analytical expression for predicting how the material from H and E will behave under strain in pile-up mode. A variety of materials from various families have been used to approve this experimental interaction. Eq. (3) shows the following expression:

$$P = E_r \left(\frac{1}{\alpha \sqrt{c}} \sqrt{\frac{E_r}{H}} + \sqrt{\frac{\pi}{4}} \sqrt{\frac{H}{E_r}} \right)^{-2} \left(h_m + h_0 \right)^2 \tag{3}$$

In Eqn. (3), we see the emergence of the coefficient α which depends on the method of Loubet et al [8-10], and the suppression of ε, a constant which depends on the geometry of the indenter in mode deformation in sink-in [11]. The coefficient c is equal to 24.5 tends to vary empirically for considerations related to the calculation of the projected contact area, and therefore the expression (3) will be slightly modified for more precision.
The aims of this research are to: 1) convert the mechanical response expression to Martens hardness in the pile-up mode; and 2) attempt to quantitatively express it as a function of the Young's modulus and, load ratio on the contact stiffness, and, considering the identification of the pile-up deformation mode and the tip defect. The proposed model is then applied to a bulk metallic material exhibiting a pile-up deformation mode, namely copper (Cu99). Additionally, the Classic Martens hardness is always calculated by multiplying the applied load by the maximum depth of indentation. This explains why this hardness is insensitive to the types of deformation under the indenter and is independent of them (sink-in or pile-up). In contrast to contact hardness (or instrumented hardness), which is proportional to the contact depth. As a result, this research is attempting to develop a semi-empirical method for determining Martens hardness that takes into account the plastic deformation of the material in pile-up mode.

THEORETICAL ASPECT

The displacement of material under the indent is a function of the mechanical properties of the material, so the profile of the indent is often useful in determining which model to use. The total indentation depth, h, is seldom equal to the indentation contact depth, hc. The two main types of topography that can occur are: the pile-up is estimated by the methodology proposed by Loubet et al. [8-10]. In the case where hc is greater than h, and the sink-in is calculated by the methodology of Oliver and Pharr [11] for hc less than h. The different physical parameters obtained from an instrumented microindentation test are presented in Figure 1.
Because of displacement of material beneath the indent is a function of the material's mechanical properties, the indent profile is frequently important in selecting which model to use. The overall depth of the indentation, h, is rarely equal to the depth of the indentation contact, hc. There are two major sorts of topography that can occur: the pile-up is

approximated using the Loubet et al. [8-10] technique. When hc is larger than h, and when hc is less than h, the sink-in is determined using the methods of Oliver and Pharr [11].
The different physical parameters obtained from an instrumented microindentation test are presented in Fig. 1.

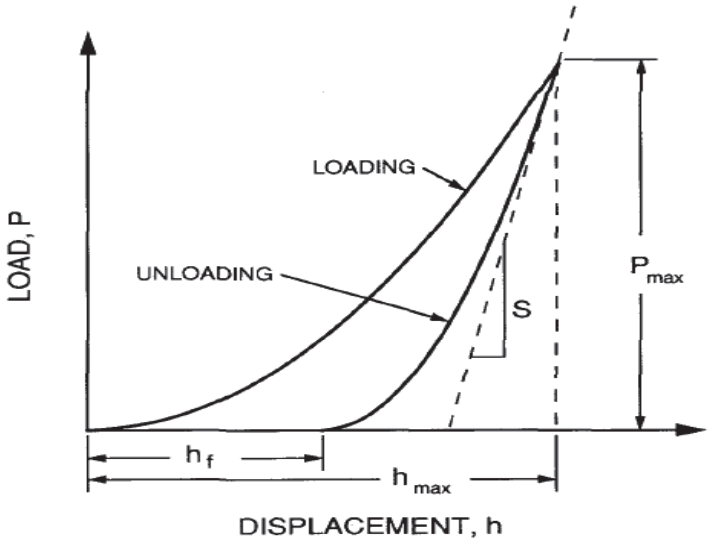

Figure 1: An instrumented indentation test's force-displacement characteristic curve.

P_{max}: Maximum force,
h_{max} = hm: maximum displacement,
h_f: residual depth,
h_r: plastic depth,
S: stiffness
h_c: contact depth.
The expression of the contact height by the model of Loubet et al. [8-10] is as follows:

$$h_c = \alpha\,(h - P/S) \tag{4}$$

To take into account the deformations around the indentation, we use the indentation hardness, H, which is defined as the ratio of the maximum applied force, P_{max}, to the projected contact surface area, A_c, at a distance h_c, which corresponds to the largest projected contact surface.

$$H = \frac{P_{max}}{A_c} \tag{5}$$

A_c is proportional to the square of the contact depth hc when employing a Vickers or Berkovich indenter with perfect geometry and can be expressed as follows:

$$A_c = 24,5h_c^2 \tag{6}$$

We use the definition of hardness H expressed in Eq. (5) to express h_c:
In Eq. (5), we express hc using the concept of hardness H:

$$h_c = \sqrt{\frac{P}{24,5H}} \tag{7}$$

In that case, S should be calculated using the unloading curve between 40 and 98 percent of the maximum load, Pmax. The following power law is frequently used:

$$P = B\left(h - h_f\right)^m \tag{8}$$

where B and m are smoothing parameters of the power law, and h_f is the final depth after total unloading of the indenter. Under these conditions, the slope S is found by taking the derivative of this function at its deepest point:

$$S = \left.\frac{dP}{dh}\right|_{h=h_{max}} = mB\left(h_{max} - h_f\right)^{m-1} \tag{9}$$

Hence, the contact stiffness is expressed as follows:

$$S = \sqrt{\frac{4}{\pi}} E_r \sqrt{A_c} \tag{10}$$

where E_r is the reduced (mixed) Young's modulus, given by:

$$\frac{1}{E_r} = \frac{1-\nu_i^2}{E_i} + \frac{1-\nu_s^2}{E_s} \tag{11}$$

with E_s and ν_s are respectively the Young modulus and Poisson's ratio of the indented sample and E_i and ν_i are those of the penetrator.

MODELING OF THE ANALYTICAL EXPRESSION $H_M - \sqrt{P/S}$ SPECIFIC TO THE PILE-UP

Transformation of Eqn. (3) according to the model of Bull and Page [12] gives:

$$\frac{P_m}{\left(h_m + h_0\right)^2} = \left(\frac{1}{\alpha\sqrt{cH}} + \frac{\sqrt{\pi H}}{2E_r}\right)^{-2} \tag{12}$$

The classic Martens hardness, H_M, expresses the ratio of the ultimate indentation load to the maximum projected area with the imposed tip defect correction as follows:

$$H_M = \frac{P_m}{A} = \frac{P_m}{26.43\left(h_m + h_0\right)^2} \tag{13}$$

Hence, we express the Martens hardness as a function of the contact hardness and the reduced modulus for the pile-up mode by combining Eqs. (12) and (13). We obtain:

$$H_M = \frac{1}{26.43}\left(\frac{1}{\alpha\sqrt{cH}} + \frac{\sqrt{\pi H}}{2E_r}\right)^{-2} \tag{14}$$

From Joslin and Oliver's relationship [13]:

$$\frac{P_m}{S^2} = \frac{\pi}{4}\frac{H_{IT}}{E_r^2} \tag{15}$$

The ratio of hardness to the square of the modulus is expressed as:

$$\frac{H_{IT}}{E_r^2}=\frac{4}{\pi}\frac{P_m}{S^2} \tag{16}$$

Finally, substituting E_r and H_{IT} by P_m/S^2 (see Eq. (16)), Eqn. (14) becomes as follows:

$$H_M=\frac{1}{26.43}\left(\frac{\sqrt{\pi}}{2\alpha\sqrt{c}}\frac{1}{\left(\frac{\sqrt{P_m}}{S}\right)E_r}+\left(\frac{\sqrt{P_m}}{S}\right)\right)^{-2} \tag{17}$$

This analytical expression is proposed in the present work for the calculation of Martens hardness as a function of the maximum indentation load, the contact stiffness and the reduced modulus of elasticity as well as two empirical constants α and c.
Note that the designation λ corresponds to the mechanical response of the primitive function H_M:

$$\lambda=\frac{1}{26.43}\left(\frac{\sqrt{\pi}}{2\alpha\sqrt{c}}\frac{1}{\left(\frac{\sqrt{P_m}}{S}\right)E_r}+\left(\frac{\sqrt{P_m}}{S}\right)\right)^{-2} \tag{18}$$

MATERIALS AND EXPERIMENTAL METHODS

In this investigation, the specimen being studied is a commercial copper of 99% purity (Cu99) and its Poisson's ratio ν=0.28. The terms in brackets are used in the following to refer to the samples. On the other hand, the objective of this work is not to deeply characterize the different tested materials from a mechanical point of view but to validate the model and the proposed methodology. That is why the authors think it is unnecessary to give more details on their microstructures to focus the readers' attention on the model. The instrumented indentation experiments were performed on samples carefully prepared to limit both the roughness at the surface and the introduction of strain hardening due to polishing. Subsequently, the specimen was grounded using SiC papers of various grit sizes and a finished by, polishing by using a series of diamond pastes until the grit size of 1 μm.
Instrumented indentation tests have been performed employing a microhardness tester CSM 2-107, equipped with a Vickers indenter (for a diamond indenter, E_i=1140 GPa and υi=0,07 [14]). The load resolution is given at 100 □ N and the depth resolution of 0.3 nm, these values being provided by the CSM Instruments Group.
At selected indentation loads ranging from 0.2 to 20 N depending on the sample, around 24 exploitable indentation tests were performed. The values of the loading and unloading rates (expressed in mN/min) were set at twice the value of the maximum applied load according to the rule proposed by Quinn *et al.*[15] and a dwell time of 15 s was imposed according to the standard indentation test procedure ASTM E92 and E384-10e2.Before analyzing the load–depth curves related to given materials, the experimental system, including both the apparatus and the sample is systematically calibrated by determining the frame compliance, C_f. Indeed, Fisher-Cripps [16] has demonstrated that this term does not have a constant value. From a mathematical point of view, this correcting factor C_f is obtained at the origin of the plot of the inverse of the total compliance as a function of the square root of the contact area. Consequently, the experimental indentation depths are corrected, following the methodology proposed by Fisher-Cripps [16], suggesting that the corrected depth is then equal to the difference between the measured depth and the product of the frame compliance to the load (in this case, C_f=0.071 nm/mN).

RESULTS AND ANALYSIS

Instrumented indentation tests for a variety of representative ultimate loadings expressed in milli-Newtons, namely 60, 125, 175, 200, 300, and 400 mN, have been produced. Fig. 2 shows the P-h loading and unloading curves:

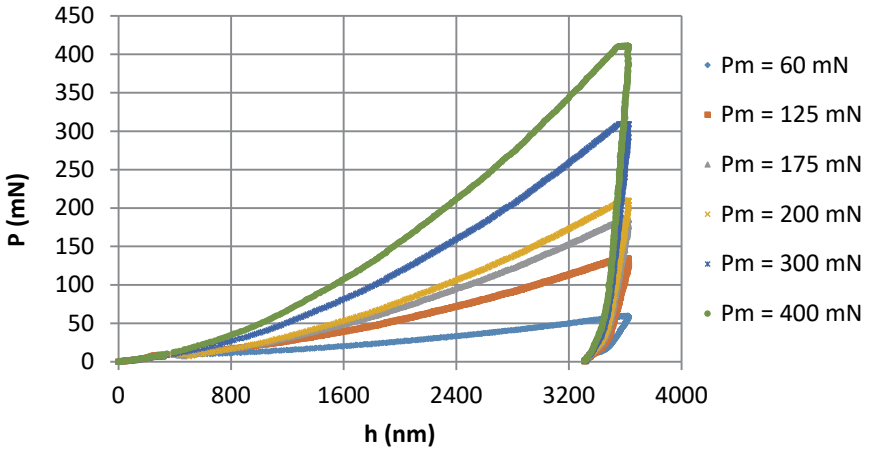

Figure 2: Characteristic curves of Cu99 at different indentation ultimate loadings.

The P-h² indentation characteristic curves of Cu99 for various indentation loads are shown in Fig. (2) which will be examined on the basis of the corrected depth, as shown in Fig. (3b). For the purpose of expressing the pile-up analytic relation according to Eq. (3) [7], we need to take into account an estimate of the tip defect, which is 150 nm in our case according to the Fischer-Cripps method [16].

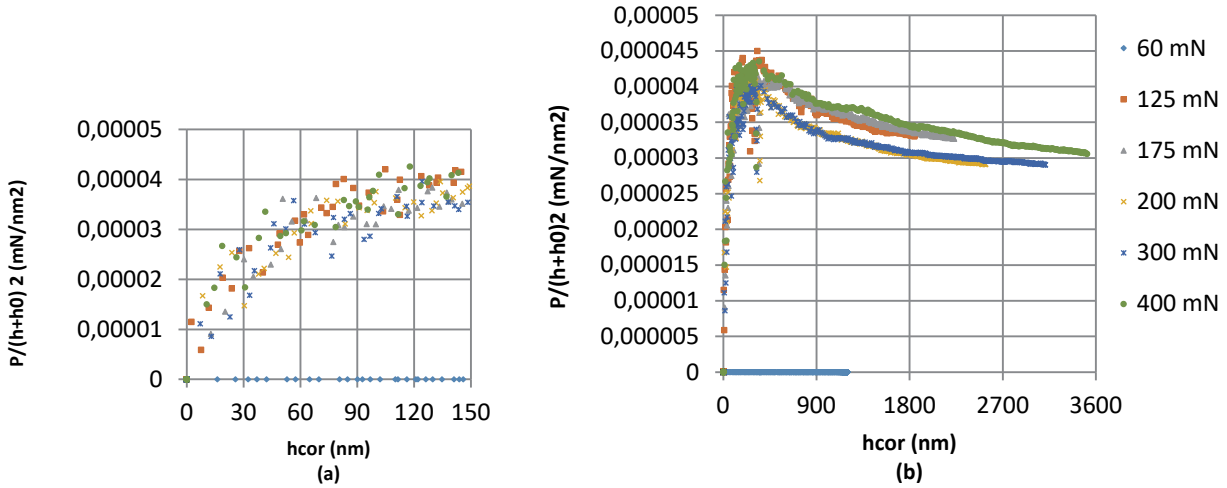

Figure 3: Graphical representation of $P/(h+h_0)^2$ as a function of the corrected depth for six ultimate loads by indentation (with h_0=150nm).

The curve (3.a) shows the evolution of the charge at low indenter penetration values. The function $P/(h+h_0)$ resultant clearly shows a decreasing trend with h [150.3600] nm (see Fig. (3.b)) and an increasing trend for shallow penetration depths ranging from 0 to 150 nm (see Fig. (3.a)). This tendency to increase this ratio at low values of penetration depths is explained by the size effect in interpretation and was discussed in a previous publication [17]. Hence, the ratio of charge to the square of the indentation depth is not constant as argued by the authors Malzbender et al. [7] in their hypotheses. This upward trend in this ratio at low penetration depth values is explained by the indentation size effect (ISE). Note that the analysis and interpretation were discussed in a previous publication [17]. Therefore, the ratio of indentation load to squared depth is not constant as mentioned by the authors Malzbender et al. [7] in their hypotheses.

In order to confirm this idea, the hardness H_M was calculated based on the indentation load P, and the stiffness based on Eq. (17) using the values of $P/(h+h_0)^2$ given in Fig. 4.
The results presented in Fig. 4, clearly show a significant dependence of the calculated hardness on the indentation load. The dependence of hardness on the measured load, ie ISE, has been widely studied and some phenomenological explanations for the origin of ISE have been proposed by the authors [18–19].

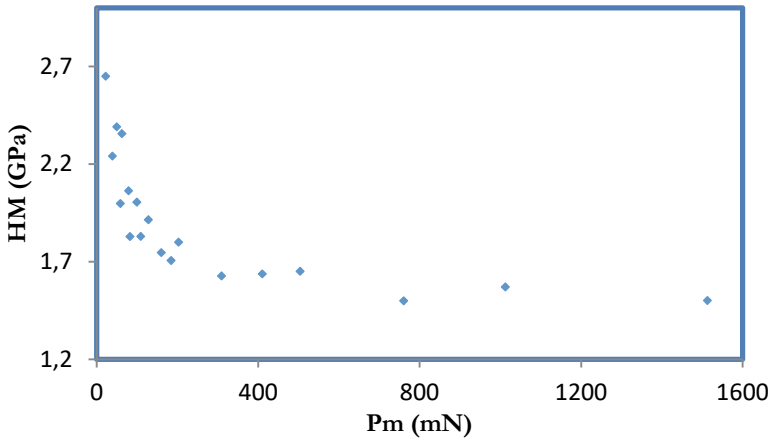

Figure 4: Graphical representation of the evolution of HM as a function of the ultimate indentation load.

The graphic representation in Fig. 4 shows a characteristic point cloud of Martens hardness expressed in GPa relating to indentation tests at maximum loads. The trend of the curve is downward from 2.7GPa to an average value equal to approximately 1.5GPa. Keep in mind that the hardness function on the ordinate is expressed in terms of the Martens hardness definition that is calculated by Eq. (14).
In order to use Eq. (17), it is necessary to identify the type of deformation mode under the indenter. From this, we calculate the ratio of the final penetration depth to the maximum depth, h_f/h_m. In our case study, the h_f/h_m ratio $=0.95\pm 0.02$, which shows that this ratio is greater than 0.83 (see details in the corresponding article [20]). Therefore, the predominant deformation mode of Cu99 is pile-up. This justifies the use of the expression (12) (see details in article [7]).
On the other hand, in the case of the expression relating to H_M compared to its response λ calculated as a function of the mixed modulus, the indentation load and the stiffness according to the expression proposed in this work, namely Eq. (17). With the correction of the maximum indenter displacements which are likely to affect all characteristic points of indentation tests as has been shown in an earlier publication [7]. Moreover, using the asymmetry correction $\beta= 1.05$ suggested by Oliver and Pharr [21].

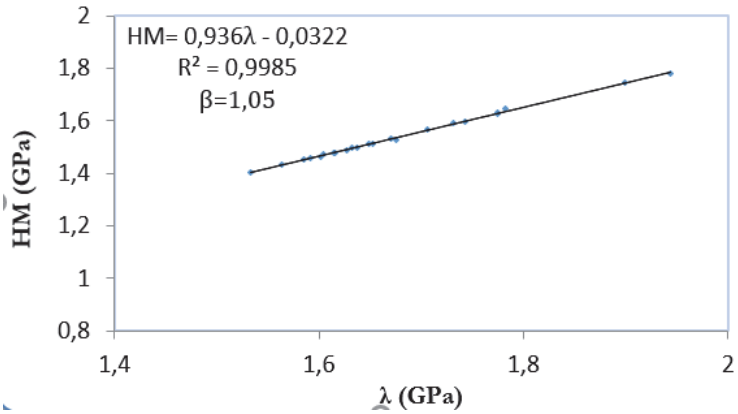

Figure 5: Representation of the evolution of H_M according to the Joslin and Oliver criterion expressed in the response λ (see Eq. (23)).

The linear regression shown in Fig. 5 shows a very good collocation of the points and a good mathematical correlation with a reproducibility rate of 99.98% which tends towards the ideal case with only 0.02% deviation. So, as can be seen, a

good linear relationship exists between the two parameters examined (the hardness function and its mechanical response), being in good agreement with the analytical expression proposed in the Eqn. (18).

CONCLUSION

On the basis of previous analysis, the following conclusion can be reached:

1. The hardness HM in Eq. (17) cannot be considered a constant. As a result, the experimentally calculated P/(h+h0)2 significantly with displacement h and the corresponding indentation load.
2. We refined an analytical expression of Martens hardness derived from a previously developed P-h^2 expression relating to pile-up [7] as a function of the $P^{1/2}/S$ criterion used by Joslin and Oliver [13] for deformation in a mode pile-up in microindentation. Martens hardness does not take into account the deformation modes under an indenter (sink-in, pile-up) which is its weak point compared to contact hardness. However, the proposed expression is a tool for predicting the variable H_M function as a function of the load, the stiffness, and the reduced modulus taking into consideration the pile-up strain mode.
3. To use this proposed expression, you only need to figure out the hf/hm ratio first. This will help you figure out the pile-up deformation mode.
4. In perspective, this experimental modeling will be generalized to the two other modes of deformations, namely the sink-in and the limit of modal coexistence.

ACKNOWLEDGEMENTS

This research was supported by the General Directorate of Scientific Research and Technological Development of Algeria (DGRSDT: Under the authority of the Ministry of Higher Education and Scientific Research in charge of scientific research).

REFERENCES

[1] Hainsworth, S. V., Chandler, H. W., Page, T. F. (1996). Analysis of nanoindentation load-displacement loading curves, J. Mater. Res., 11, pp. 1987-1995. DOI: 10.1557/JMR.1996.0250.

[2] Loubet, J. L., Georges, J. M., Meille, J. (1986). In Microindentation Techniques in Materials Science and Engineering, edited by P. J. Blau and B. R. Lawn (American Society for Testing and Materials, Philadelphia), pp. 72–89.

[3] Zeng, K., Rowcliffe, D. (1996). Analysis of penetration curves produced by sharp indentations on ceramic materials, Philosophical Magazine A 74, pp. 1107-1116. DOI: 10.1080/01418619608239711.

[4] Cheng, Y.-T., Cheng, C.-M. (1998). Relationships between hardness, elastic modulus, and the work of indentation, Appl. Phys. Lett., 73, p. 614. DOI: 10.1063/1.121873.

[5] Sun,Y., Zheng, S., Bell, T., Smith, J. (1999). Indenter tip radius and load frame compliance calibration using nanoindentation loading curves, Philosophical Magazine Letters 79, pp. 649-658. DOI: 10.1080/095008399176698

[6] Malzbender, J., de With, G., den Toonder, J. (2001). The P–h^2 relationship in indentation, J. Mater. Res. 15, pp. 1209-1212. DOI: 10.1557/JMR.2000.0171.

[7] Habibi, S., Chicot, D., Mejias, A., Boutabout, B., Zareb, E., Semsoum, D.-E., Benaissa, S., Mezough, A., Merzouk H. (2021). The P–h^2 relationship on load–displacement curve considering pile-up deformation mode in instrumented indentation, Journal of Materials Research, 36, pp. 3074–3085. DOI: 10.1557/s43578-021-00286-3.

[8] Loubet, J.L., Bauer, M., Tonck, A., Gauthier Manuel, B. (1993). Nanoindentation with a surface force apparatus, Mechanical properties and deformation behaviour of materials having ultra-fine microstructures, Kluwer Academic Publishers 233, pp. 429-447.

[9] Guillonneau, G. et al. (2012). Determination of mechanical properties by nanoindentation independendly of indentation depth measurement. Journal of Materials Research, 27, pp. 2551-2560. DOI: 10.1557/jmr.2012.261

[10] Bec, S., Tonck, A., Georges, J-M., Georges, E., Loubet, J.-L. (1996). Improvements in the indentation method with a surface force apparatus, Philos. Mag., A 74, p. 1061. DOI: 10.1080/01418619608239707.

[11] Oliver, W.C. and Pharr, G.M. (1992). An improved technique for determining hardness and elastic modulus using load and displacement sensing indentation experiments, J. Mater. Res., 7, pp. 1564-1583.

DOI: 10.1557/JMR.1992.1564.
[12] Bull, S. J., Page, T. F., Yoffe, E. H. (1989). An explanation of the identification size effect in ceramics, Philos. Mag. Lett., 59, pp. 281–288. DOI: 10.1080/09500838908206356.
[13] Joslin, D.L., Oliver, W. C. (1990). A new method for analyzing data from continuous depth-sensing microindentation tests, J. Mater. Res., 5. DOI: 10.1557/JMR.1990.0123.
[14] Field, J.-E., Telling, R.-H. (1999). The Young modulus and Poisson ratio of diamond, Research Note Cambridge, Cavendish Laboratory.
[15] Quinn, G.-D., Patel, P.-L., Loyd, I. (2002). Effect of loading rate upon conventional ceramic microindentation hardness, J. Res. Natl. Inst. Stand. Technol., 107, pp. 299–306. DOI: 10.6028/2Fjres.107.023.
[16] Fischer-Cripps, A.-C. (2006). Critical review of analysis and interpretation of nano-indentation test data. Surf. Coat. Technol. 200, pp. 4153–65. DOI: 10.1016/j.surfcoat.2005.03.018.
[17] Soufiane, B., Habibi, S., Semsoum, D.-E., Merzouk, H., Mezough, A., Boutabout, B., Montagne, A. (2021). Exploitation of static and dynamic methods for the analysis of the mechanical nanoproperties of polymethylmetacrylate by indentation, Frattura ed Integrità Strutturale, 56, pp. 46-55. DOI: 10.3221/IGF-ESIS.56.03.
[18] Fröhlich, F., Grau, P., Grellmann, W. (1977). Performance and analysis of recording microhardness tests, Phys. Stat. Sol. (a), 42, pp. 79–89. DOI: 10.1002/pssa.2210420106.
[19] Li, H., Bradt, RC. (1993). The microhardness indentation load/size effect in rutile and cassiterite single crystals, J. Mater. Sci., 28, pp. 917–926. DOI: 10.1007/BF00400874.
[20] Yetna N'Jock, M., Chicot, D., Ndjaka, J.-M., Lesage, J., Decoopman, X., Roudet, F., and Mejias, A. (2015). A criterion to identify sinking-in and piling-up in indentation of materials, Int. J. Mech. Sci., 90, pp. 145-150. DOI: 10.1016/j.ijmecsci.2014.11.008.
[21] Oliver, W.C., Phar, G.M. (2004). Measurement of hardness and elastic modulus by instrumented indentation: Advanced in understanding and refinements to methodology, J. Mat. Res., 19, pp. 3-20. DOI: 10.1557/jmr.2004.19.1.3.